Exact equilibrium crystal shapes in two dimensions for free-fermion models

Mark Holzer*
Department of Physics, Simon Fraser University, Burnaby, British Columbia, Canada V5A 1S6
(Received 9 May 1990)

Using a conceptually novel approach that maps a two-dimensional interface exactly onto a Feynman-Vdovichenko lattice walker, we derive an exact and general solution for the equilibrium crystal shapes (ECS's) of free-fermion models, i.e., models that are solvable via the Feynman-Vdovichenko or (equivalently) Pfaffian methods. The ECS for these models is given by the locus of purely imaginary poles of the determinant of the "momentum-space" lattice-path propagator. The ECS may, therefore, simply be read off from the analytical expression for the bulk free energy. From these shapes one can then obtain numerically (but to arbitrary accuracy) the high-temperature direction-dependent correlation length of the dual system. We give several examples of previously unknown Ising ECS's, and we examine in detail the free-fermion case of the eight-vertex model. The free-fermion eight-vertex model includes the modified potassium dihydrogen phosphate (KDP) model, which is not in the Ising universality class. The ECS of the modified KDP model is shown to be the limiting case of the ECS of an antiferromagnetic 2×1 phase on a triangular lattice in the limit of infinite interactions. The ECS of the modified KDP model is lenticular at finite temperature and has sharp corners. We explain the physics of this lens shape from an elementary calculation.

I. INTRODUCTION

When a system is at solid-fluid coexistence, a macroscopic crystal can coexist in equilibrium with the surrounding "sea" of fluid. Because of the anisotropy of the crystal-fluid interfacial free energy per unit area, the crystal has an interesting temperature- (T) dependent shape, the so-called equilibrium crystal shape (ECS). In a broader sense, the ECS is the shape of any macroscopic inclusion of one phase in another, when the two phases coexist in equilibrium. While the thermodynamics of ECS's has been understood for nearly a century,[1] the determination of these shapes from the statistical mechanics of a microscopic Hamiltonian has been a problem of considerable interest only in recent years.[2] The Ising model in zero magnetic field and below the bulk transition temperature (T_c) is the simplest model describing the full two-phase system [as opposed to a pure "interface" model such as the solid-on-solid (SOS) model[3]]. The two-dimensional (2D) Ising model is particularly interesting for at least two reasons: (1) Exact solutions are possible[4-6] and (2) these exact solutions are valuable in approximating the shapes of facets of 3D Ising ECS's.[7,8] Since some real crystals, such as noble-gas crystals, may possibly be approximated by an appropriate Ising model, 2D Ising ECS's may also have some relevance to the analysis of experimental facet-shape data.[8]

In a recent Letter,[9] we gave a general exact solution for the equilibrium crystal shapes of 2D Ising models with noncrossing bonds. This solution immediately generalizes to the somewhat larger class of free-fermion models, which includes non-Ising models and is the class of all models for which the bulk free energy may be found exactly by the Feynman-Vdovichenko[10,11] (FV) (or equivalently by the Pfaffian[12]) method. The central result of Ref. 9 is that the ECS is given by the locus of purely imaginary poles of the determinant of the lattice-path propagator. To be precise, if the "momentum-space" FV lattice-walk matrix for a lattice $\mathcal{L}^*$ (the dual of the direct lattice $\mathcal{L}$) is denoted by $\mathbf{\Lambda}(k_x,k_y)$, then the ECS for the dual model on $\mathcal{L}$, represented in Cartesian coordinates as $Y(X)$, is given by

$$\mathrm{Det}[\mathbf{1}-\mathbf{\Lambda}(k_x=i\beta\lambda Y,k_y=-i\beta\lambda X;\{\omega\})]=0,\quad T<T_c\ , \tag{1}$$

where $\{\omega\}$ denotes the set of Boltzmann weights associated with the steps of the lattice walk. The matrix $\mathbf{\Lambda}$ is a finite-dimensional $q\times q$ matrix, where q is even and, in the simplest cases, just equal to the coordination number of the lattice. Since the bulk partition function of free-fermion models can be expressed in terms of an integral $\int dk_x \int dk_y \ln \mathrm{Det}(\mathbf{1}-\mathbf{\Lambda})$ (Refs. 10, 11, and below), the ECS's for these models may, in fact, be read off from the analytic form of the bulk free energy!

It is the purpose of this paper to give a more detailed derivation of this simple result, to give some examples of previously unknown Ising ECS's, and to explore, in some detail, a pedagogical example of a non-Ising case for which Eq. (1) is also valid. The remainder of this paper is organized as follows: In Sec. II we derive Eq. (1) and discuss its practical use and range of validity. In Sec. III we apply the FV method to the free-fermion cases of the eight-vertex model.[13-15] We identify the coexisting phases of the model and show that Eq. (1) gives the correct ECS of the corresponding dual models even for the non-Ising case of the modified potassium dihydrogen phosphate (KDP) model.[16,17] In Sec. IV we conclude.

II. GENERAL SOLUTION

For definiteness consider an Ising model with ferromagnetic interactions. The generalization to other

free-fermion models is immediate and will be made at the end of this section. Let the 2D Ising system be defined on a rectangular strip Ω of a planar lattice $\mathcal{L}$, i.e., a lattice with noncrossing bonds. The strip Ω has a geometric dual, the strip Ω^* of the dual lattice $\mathcal{L}^*$. Without loss of generality, we take the lattice to have basis vectors $\hat{\mathbf{x}}$ and $\hat{\mathbf{y}}$, and we align the strip with the y axis. (It is always possible to choose a coordinate system in which the basis vectors of the lattice are orthogonal unit vectors.) We take the width of Ω^* to be N and think of the length of Ω^* as finite, but tending toward infinity (Fig. 1). At zero magnetic field and $T<T_c$, a phase of predominantly "up" (+) spins can coexist with a phase of predominantly "down" (−) spins. The microscopic configurations of the system can of course be described in terms of the spins on Ω, but in the present context it is much more useful to think in terms of the bonds of Ω^* dual to the "broken" bonds of Ω which connect spins of opposite sign. We consider these bonds to be elementary microscopic interfaces of microscopic normal $\hat{n}$, which we take to point from − to +. If the coupling between spins at sites i and j of Ω is K_{ij}, the creation of an elementary interface between them costs energy $2K_{ij}/\beta$ and is, therefore, associated with a Boltzmann factor of $\omega_{ij}=\exp(-2K_{ij})$, where $\beta\equiv(k_BT)^{-1}$, with k_B Boltzmann's constant.

A macroscopic interface between the (+) phase and the (−) phase can be forced into the system by dividing the boundary of Ω into two connected (1D) regions and fixing the boundary spins in one region to be + and in the other region to be −. As shown in Fig. 1, this forces an interface to run across the strip from the dual spin $\sigma^*_{(0,0)}$ at (0,0) to the dual spin $\sigma^*_{(N,M)}$ at (N,M) on the boundary of Ω^*. With this (+ −) choice of boundary condition, denote the Hamiltonian of the system by $\mathcal{H}^{+-}_{N,M}$ and its partition function by $Z^{+-}_{N,M}=\mathrm{Tr}\exp(-\beta\mathcal{H}^{+-}_{N,M})$. If all boundary spins are fixed to be +, denote the Hamiltonian of the system by $\mathcal{H}^{++}$ and its partition function by $Z^{++}=\mathrm{Tr}\exp(-\beta\mathcal{H}^{++})$. In the latter case, there can be no macroscopic interface across the strip, which now contains only the pure + phase. The sample free energy $\beta F^{++}=-\ln Z^{++}$ contains contributions from the bulk and from the boundaries, only. The sample free energy $\beta F^{+-}=-\ln Z^{+-}_{N,M}$ contains contributions form the bulk, from the boundaries, and from the interface running from (0,0) to (N,M). The interfacial free energy per unit length, $\gamma(\hat{\mathbf{n}})$, for an interface of macroscopic orientation $\hat{\mathbf{n}}$ is thus naturally defined by the thermodynamic limit

$$\beta\gamma(\hat{\mathbf{n}})\equiv-\lim_{L\to\infty}\frac{1}{L}\ln\left[\frac{Z^{+-}_{N,M}}{Z^{++}}\right] \tag{2}$$

$$=-\lim_{L\to\infty}\frac{1}{L}\ln\langle\sigma^*_{(0,0)}\sigma^*_{(N,M)}\rangle=1/\xi^*(\hat{\mathbf{u}})\ , \tag{3}$$

where $L\equiv(N^2+M^2)^{1/2}$, $\hat{\mathbf{n}}=(-M,N)/L$, $\hat{\mathbf{u}}=(N,M)/L$, and $\xi^*(\hat{\mathbf{u}})$ is the high-T correlation length of the dual system in the $\hat{\mathbf{u}}$ direction, with $\hat{\mathbf{n}}\cdot\hat{\mathbf{u}}=0$. We will use the convention that $N>0$ ($N<0$) corresponds to the upper (lower) half of the strip being in the (+) phase and the lower (upper) half in the (−) phase. The duality statement of Eq. (3) has been derived by a number of authors[18] and forms the basis of all solutions[4,5] which were known prior to our result Eq. (1): A calculation of the dual-lattice correlations $\langle\sigma^*_{(0,0)}\sigma^*_{(N,M)}\rangle$ in the thermodynamic limit $N,M\to\infty$, with $\hat{\mathbf{n}}$ ($\hat{\mathbf{u}}$) fixed, gives $\gamma(\hat{\mathbf{n}})$, from which the ECS is determined via the well-known Wulff construction.[1] We call this the "canonical" formulation of the ECS problem, because the interfacial free energy must first be calculated from Eq. (2) at *fixed* macroscopic orientation.

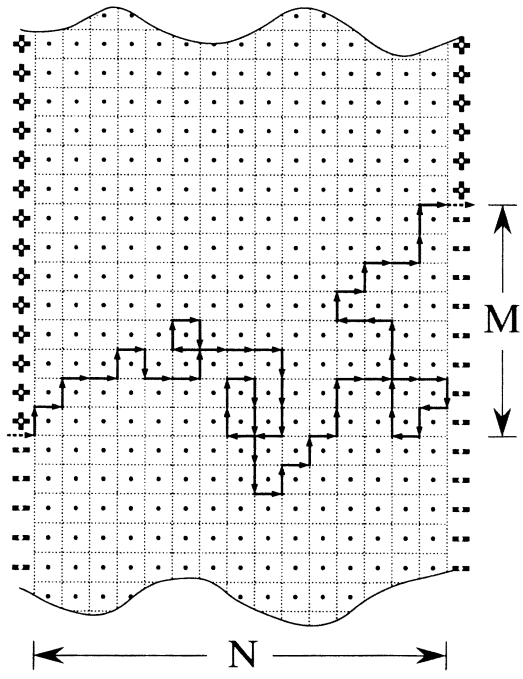

FIG. 1. Boundary conditions considered in this paper, illustrated on a rectangular lattice: The strip Ω of the square lattice $\mathcal{L}$ is defined by the heavy dots, and the spins on its boundary are forced to be either "up" (+) or "down" (−) as shown. Its dual, the strip Ω^* of the dual lattice $\mathcal{L}^*$, is indicated by the grid of dotted lines. The (+ −) boundary conditions force an interface into the system, which runs from dual spin $\sigma^*_{(0,0)}$ to dual spin $\sigma^*_{(N,M)}$. The lattice walk shown illustrates a term in the sum of Eq. (9).

In this paper we shall take an alternative approach, which allows the direct determination of the ECS from statistical mechanics, without going through the auxiliary function $\gamma(\hat{\mathbf{n}})$. One of the key results in the theory of ECS's is that the ECS can be regarded as the "grand canonical" form of the interfacial free energy, that is, the ECS is the Legendre transform of the "canonical" interfacial free energy $\gamma(\hat{\mathbf{n}})$.[19] This statement takes a particularly simple form if the ECS is represented in Cartesian coordinates as (in 2D) $Y(X)$:

$$\lambda Y(X)=f(s)+\lambda Xs,\quad \lambda X=-\frac{\partial f}{\partial s},\quad s=\frac{\partial Y}{\partial X}\ , \tag{4}$$

where $f(s)\equiv\gamma(\hat{\mathbf{n}})(1+s^2)^{1/2}$, $\hat{\mathbf{n}}=(-s,1)/(1+s^2)^{1/2}$, and λ is a constant controlling the volume of the ECS. In going from $f(s)$ [or $\gamma(\hat{\mathbf{n}})$] to $Y(X)$, we pass from a "canonical" ensemble at fixed macroscopic slope s (or $\hat{\mathbf{n}}$) (the density variable) to a "grand canonical" ensemble, in which all s are allowed and X (the field variable) selects a particular slope s as $\partial Y/\partial X$. We may, therefore, express the ECS in terms of a grand canonical trace as[20]

$$\beta\lambda Y(X)=\lim_{|N|\to\infty}\frac{1}{N}\left\{-\ln\sum_{M}\mathrm{Tr}\exp\left[-\beta\left[\mathcal{H}^{+-}_{N,M}-\lambda X\hat{\mathbf{x}}\cdot\sum_{i}\hat{\boldsymbol{n}}_i d_i\right]\right]-\beta F^{++}\right\}, \tag{5}$$

where the sum in the exponential extends over all microscopic interfaces whose length and normal are denoted by d_i and $\hat{\boldsymbol{n}}_i$. In Eq. (5) the local density variable $\hat{\boldsymbol{n}}_i$ has been coupled to the field variable $\lambda X\hat{\mathbf{x}}$ and the sum over M sums over an ensemble of systems of all possible macroscopic interface orientations. We take each system of this ensemble to be defined on Ω with $+$ $-$ boundary conditions labeled by M. The sum $\sum_i \hat{\boldsymbol{n}}_i d_i$ vanishes around microscopic interfaces forming closed loops. Thus, the only contributions to the field term in the exponent arise from the line from (0,0) to (N,M), and that contribution is $-\lambda X\hat{\mathbf{x}}\cdot\sum_i \hat{\boldsymbol{n}}_i d_i=\lambda XM$, independent of the particular path traced out by the line. Thus, Eq. (5) becomes

$$\beta\lambda Y(X)=-\lim_{|N|\to\infty}\frac{1}{N}\ln\sum_{M}e^{-\beta\lambda XM}\left[\frac{Z^{+-}_{N,M}}{Z^{++}}\right]. \tag{6}$$

The field term $\exp(-\beta\lambda XM)$ is a fugacity for the "height" M and, therefore, controls the orientation of the interface. We now evaluate $Z^{+-}_{N,M}/Z^{++}$ using the Vdovichenko-Feynman "random walker" method.[10,11]

To see what the interface has to do with walkers, consider the standard low-T expansions[21] of $Z^{+-}_{N,M}$ and Z^{++}:

$$Z^{++}=e^{-\beta E_0}\sum_{\{G\}_{++}}W(G)\equiv e^{-\beta E_0}\Sigma_{++} \tag{7}$$

$$Z^{+-}_{N,M}=e^{-\beta E_0}\sum_{\{G\}_{+-}}W(G)\equiv e^{-\beta E_0}\Sigma_{+-}. \tag{8}$$

In Eqs. (7) and (8), E_0 is the ground-state energy of the system with the $(++)$ boundary condition, $\{G\}_{++}$ is the set of graphs which can be drawn on Ω^* such that each graph is equivalent to a configuration of elementary interfaces when the $(++)$ boundary condition is imposed, $\{G\}_{+-}$ is the corresponding set of graphs for the $(+\ -)$ boundary condition, and each graph is summed with weight $W(G)$. Since each link of a graph G corresponds to an elementary interface, the weight of G is given by $W(G)=\prod_{\text{links}}\omega_{ij}$, where the product is taken over all the links of G. The set $\{G\}_{++}$ contains closed polygons (loops) only. The set $\{G\}_{+-}$ contains loops and open graphs connecting (0,0) and (N,M). If $(\bigcirc)$ denotes the sum of $W(G)$ over all single closed loops, $(\bigcirc\sim\bigcirc)$ the sum over all pairs of closed loops, $(-)$ the sum over the open graphs, $(-\sim\bigcirc)$ the sum over open graphs in the presence of single closed loops, etc., we can write, symbolically,

$$\Sigma_{++}=1+(\bigcirc)+(\bigcirc\sim\bigcirc)+\cdots,$$

$$\Sigma_{+-}=(-)+(-\sim\bigcirc)+(-\sim\bigcirc\sim\bigcirc)+\cdots.$$

Instead of evaluating the sums over closed loops, it turns out to be easier (as first conjectured by Kac and Ward,[22] first utilized by Feynman,[11] and finally proved by Sherman[23]) to sum over closed *directed* lattice paths (lattice walks). Give weight $W(\vec{G})=(-1)^S\prod_{\text{steps}}\omega_{ij}$ to each single directed closed path $\vec{G}$, where S is the number of self-intersections of the path and the product is over the steps (directed links) of the path. The upshot of the Sherman theorem,[23] which holds for any planar embedded lattice with noncrossing bonds, is that $\Sigma_{++}=\exp(\bigcirc)$, where $(\bigcirc)$ denotes the sum of $W(\vec{G})$ over all possible $\vec{G}$. The crucial point here is that the n-loop term of the directed paths has uncoupled into $(\bigcirc)^n/n!$ Hence, if $(-)$ denotes the sum over open graphs which are counted using directed paths weighted in the same manner as the closed paths of $(\bigcirc)$, one is led to expect that $(-)$ uncouples from the $(\bigcirc)$'s so that, $Z^{+-}_{N,M}=(-)Z^{++}$. Calheiros, Johannesen, and Merlini[24] showed that, indeed, this follows rigorously from the Sherman theorem by considering the closed-loop expansion with an auxiliary bond J_a^* external to $\mathcal{L}^*$ connecting the dual sites (0,0) and (N,M). In the limit as $J_a^*\to 0$, one finds that[25]

$$\frac{Z^{+-}_{N,M}}{Z^{++}}=\sum_{(0,0)\to(N,M)}(-1)^S\prod_{\text{steps}}\omega_{ij}, \tag{9}$$

where the sum extends over all directed paths from (0,0) to (N,M), the product is over all directed links or steps of the path, and S is the number of self-intersections of the path.

Following Feynman[11] and Vdovichenko,[10] the sum of Eq. (9) can now easily be evaluated, at least in the thermodynamic limit as $|N|\to\infty$. Let $\{\mathbf{d}_\mu\}$, with $\mu\in\{1,2,\ldots,q\}$, be the set of vectors which correspond to all possible distinct directed bonds of $\mathcal{L}^*$. If $\mathcal{L}^*$ is a Bravais lattice, q is the coordination number; otherwise, q is the sum of the coordination numbers for each site of the unit cell. (Since for each $\mathbf{d}_\mu$ there is a $\mathbf{d}_\nu=-\mathbf{d}_\mu$, q is even.) Imagine the paths from (0,0) to (N,M) to be generated by a lattice walker and denote by $\mathbf{d}_\mu(n)$ the nth step of the walk. With each change of the walker's direction, we associate a phase factor $\exp(i\phi_{\mu\nu}/2)$, where $\phi_{\mu\nu}$ is the angle ("of turn") from $\mathbf{d}_\nu(n)$ to $\mathbf{d}_\mu(n+1)$, defined such that $|\phi_{\mu\nu}|<\pi$. ($|\phi_{\mu\nu}|=\pi$ will be excluded explicitly.) This keeps track of the parity of self-intersections because the product of these phase factors over a single closed loop gives $-(-1)^S$, a topological property of planar embedded loops.[22,26] Let $\Psi_{\mu\kappa}(x,y;n)$ be the sum over all weighted walks (including the phase factors) which step onto the origin with $\mathbf{d}_\kappa(0)$ and n steps later, onto site (x,y) with $\mathbf{d}_\mu(n)$. These $\Psi_{\mu\kappa}(x,y;n)$ then obey a recursion equation which, in the limit as the strip width $|N|\to\infty$ and full translational symmetry is restored, can be diagonalized via a Fourier transform to obtain[10,11]

$$\Psi_{\mu\kappa}(k_x,k_y;n+1)=\sum_{\nu}\Lambda_{\mu\nu}(k_x,k_y)\Psi_{\nu\kappa}(k_x,k_y;n). \tag{10}$$

The $\Lambda_{\mu\nu}$ are the elements of the $q\times q$ matrix $\boldsymbol{\Lambda}$ and have the form

$$\Lambda_{\mu\nu}(k_x,k_y;\omega_{ij})=\omega_{ij}e^{i\phi_{\mu\nu}/2}e^{-i\mathbf{k}\cdot\mathbf{d}_\mu}(1-\delta_{\mathbf{d}_\mu,-\mathbf{d}_\nu}), \tag{11}$$

where $\mathbf{k}=(k_x,k_y)$. The Kronecker δ in (11) ensures that walks cannot immediately backtrack ($|\phi_{\mu\nu}|=\pi$). The sum over all paths from (0,0) to (N,M), [Eq. (9)] can now be written in terms of $\mathbf{\Lambda}$ as[27]

$$\frac{Z^{+-}_{N,M}}{Z^{++}}=\int\int_{-\pi}^{\pi}\frac{dk_x dk_y}{(2\pi)^2}e^{i(k_xN+k_yM)}\sum_{m=0}^{\infty}(\mathbf{\Lambda}^m)_{\mu_{\rm out}\nu_{\rm in}}\ . \tag{12}$$

In principle, the strip Ω should be chosen such that $\mu_{\rm out}=\nu_{\rm in}$, and so self-intersections are properly accounted for; however, in the thermodynamic limit this is not important, since we can then replace $(\mathbf{\Lambda}^m)_{\mu_{\rm out}\nu_{\rm in}}$ with $\mathrm{Tr}(\mathbf{\Lambda}^m)$.

The FV method gives us an intuitive picture of a walker, described by the step-to-step transition matrix $\mathbf{\Lambda}$, generating all possible interface configurations. While $\mathbf{\Lambda}$ cannot keep track of the microscopic interface orientations, the field term of Eq. (6) can be incorporated into $\mathbf{\Lambda}$ because it depends only on the y coordinate M of the final step of the walk. Since with every transition to a step $\mathbf{d}_\mu$ the walker's y coordinate changes by $\hat{\mathbf{y}}\cdot\mathbf{d}_\mu$, we can associate with this transition a field term $\exp(-\beta\lambda X\hat{\mathbf{y}}\cdot\mathbf{d}_\mu)$ in addition to the topological phase factor and the Boltzmann weight. The product of these field-term factors over the path from (0,0) to (N,M) gives a total field term of $\exp(-\beta\lambda XM)$. Diagonalizing the corresponding recursion equations, one arrives (trivially) at the same form of $\mathbf{\Lambda}$ as in the case $X=0$ except that where we used to have just k_y, we now have $k_y-i\beta\lambda X$. Thus, $(Z^{+-}_{N,M}/Z^{++})\exp(-\beta\lambda XM)$ is simply given by the right-hand side of (12) except that $\mathbf{\Lambda}(k_x,k_y)$ is replaced with $\mathbf{\Lambda}(k_x,k_y-i\beta\lambda X)$. Substituting this form of $(Z^{+-}_{N,M}/Z^{++})\exp(-\beta\lambda XM)$ into Eq. (6), we obtain[28]

$$\beta\lambda Y(X)=-\lim_{|N|\to\infty}\frac{1}{N}\ln\left[\sum_{M=-\infty}^{+\infty}\int\int_{-\pi}^{\pi}\frac{dk_x dk_y}{(2\pi)^2}e^{i(k_xN+k_yM)}\mathrm{Tr}(\mathbf{1}-\mathbf{\Lambda})^{-1}\right], \tag{13}$$

where $\mathbf{\Lambda}=\mathbf{\Lambda}(k_x,k_y-i\beta\lambda X)$ and X must be bounded such that $\mathbf{\Lambda}^P\to\mathbf{0}$ as $P\to\infty$. Summing over M, using the identity $\sum_{M=-\infty}^{+\infty}\exp(ik_yM)=2\pi\sum_{n=-\infty}^{+\infty}\delta(k_y-2\pi n)$, and then integrating over k_y, we obtain

$$\beta\lambda Y(X)=-\lim_{|N|\to\infty}\frac{1}{N}\ln\left[\int_{-\pi}^{\pi}\frac{dk_x}{2\pi}e^{ik_xN}\frac{\sum_{l=1}^{q}\prod_{j\neq l}^{q}(1-\lambda_j)}{\mathrm{Det}(\mathbf{1}-\mathbf{\Lambda})}\right], \tag{14}$$

where $\mathbf{\Lambda}=\mathbf{\Lambda}(k_x,-i\beta\lambda X)$ and λ_l, with $i\in\{1,\ldots,q\}$, denote the eigenvalues of $\mathbf{\Lambda}$. In the thermodynamic limit $|N|\to\infty$, only the saddle point contributes to the integral of Eq. (14). With $\mathbf{\Lambda}$ of the form (11), the condition for the integrand of (14) to have a saddlepoint[29] is given by $\mathrm{Det}(\mathbf{1}-\mathbf{\Lambda})=0$, which is approached asymptotically like $1/N$, i.e., $\mathrm{Det}(\mathbf{1}-\mathbf{\Lambda})\to0$ like $1/N$ as $|N|\to\infty$. Thus (14) is simply evaluated as

$$\beta\lambda Y(X)=-i\bar{k}_x\ , \tag{15}$$

where $\bar{k}_x$ is the solution to $\mathrm{Det}[\mathbf{1}-\mathbf{\Lambda}(\bar{k}_x,-i\beta\lambda X)]=0$, which may succinctly be expressed in the form of Eq. (1). The propagator for lattice paths is defined as the amplitude for the walker to arrive after any number of steps, i.e., as $\sum_{m=0}^{\infty}\mathbf{\Lambda}^m=(\mathbf{1}-\mathbf{\Lambda})^{-1}$. Equation (1), therefore, expresses the ECS as the locus of purely imaginary poles of the determinant of the propagator for lattice paths.

An alternative way of evaluating (13) is to make use of the fact that replacing $\mathrm{Tr}(\mathbf{1}-\mathbf{\Lambda})^{-1}$ with $1/\mathrm{Det}(\mathbf{1}-\mathbf{\Lambda})$ in the integrand of (13) does not change the saddle point in the thermodynamic limit $|N|\to\infty$. This allows us to obtain further insight into the analytical structure of solution (1). Replacing $\mathrm{Tr}(\mathbf{1}-\mathbf{\Lambda})^{-1}$ with $1/\mathrm{Det}(\mathbf{1}-\mathbf{\Lambda})$, summing over M, integrating over k_y, and making the change of variable $e^{ik_x}=z$ leaves us with the contour integral

$$\beta\lambda Y(X)=-\lim_{|N|\to\infty}\frac{1}{N}\ln\left[\oint\frac{dz}{2\pi i}\frac{z^N}{z\,\mathrm{Det}(\mathbf{1}-\mathbf{\Lambda})}\right], \tag{16}$$

where $\mathbf{\Lambda}=\mathbf{\Lambda}(k_x,-i\beta\lambda X)$ and the contour of integration is counter clockwise around the unit circle $|z|=1$. Since for matrices $\mathbf{\Lambda}$ of the form (11), the translational invariance of the lattice implies that $\mathrm{Det}(\mathbf{1}-\mathbf{\Lambda})$ is just a polynomial in z and $1/z$ (see also Ref. 29), the result [Eq. (15)] follows immediately. For all the Ising models of Ref. 30 for which the exact (bulk) solution is known, the poles of the integral of Eq. (16) have a very simple structure: For all these models $z\,\mathrm{Det}(\mathbf{1}-\mathbf{\Lambda})$ is of the form $[z-z_1(X)][z-z_2(X)]$ for appropriate orientation of the axes. The roots $z_1(X)$ and $z_2(X)$ are real and positive for $X\in[X_{\rm min},X_{\rm max}]$ and $T<T_c$. For a range of the field variable $X\in[X_A,X_B]\subset[X_{\rm min},X_{\rm max}]$, $z_1(X)\le1$, and $z_2(X)\ge1$. Thus, for $X\in[X_A,X_B]$, Eq. (16) is evaluated as $\beta\lambda Y(X)=-\ln[z_1(X)]$, if $N>0$, and as $-\ln[z_2(X)]$, if $N<0$. Since the outward normal of the interface is $\hat{\mathbf{n}}=(-\langle M\rangle(X),N)/L$, $N>0$ ($N<0$) corresponds to the "upper (lower) half" of the ECS. If $X_A\neq X_{\rm min}$ and $X_B\neq X_{\rm max}$, and $X\in[X_{\rm min},X_A]\cup[X_B,X_{\rm max}]$, then (by definition) either both or neither of the poles z_1,z_2 lie inside $|z|=1$. In this case we find that $\mathbf{\Lambda}^P(k_x,k_y-i\beta\lambda X)$ no longer converges for all real (k_x,k_y) as $P\to\infty$.

Hence, for $X\in[X_{\min},X_A]\cup[X_B,X_{\max}]$, the substitution $\mathbf{\Lambda}(k_x,k_y)\rightarrow\mathbf{\Lambda}(k_x,k_y-i\beta\lambda X)$, which incorporates the field term of Eq. (6) into $\mathbf{\Lambda}$, is no longer well founded mathematically for a purely real integration path in the k_x plane. However, since the ECS of any 2D system with finite, short-range forces is smooth[2,4,5] for $0<T<T_c$, it follows from *analytical continuity* that the upper half of the ECS must be given by $-\ln[z_1(X)]$, and the lower half by $-\ln[z_2(X)]$, for the *entire* range of field $X\in[X_{\min},X_{\max}]$. This analytical continuation amounts to deforming the integration contour of Eq. (16) to include the relevant pole, thereby avoiding regions in the z plane (k_x plane) where the modulus of one or more eigenvalues of $\mathbf{\Lambda}(k_x,-i\beta\lambda X)$ is greater or equal to unity. [In writing down the integral as its saddle point as in Eq. (15), this analytical continuation is implicit.] In general, the ECS problem is defined for those fields X that allow a path in the k_x plane from $-\pi$ to π along which the modulus of every eigenvalue of $\mathbf{\Lambda}(k_x,-i\beta\lambda X)$ remains less than unity. To summarize, we have for $T<T_c$ and $X_{\min}\le X\le X_{\max}$

$$\beta\lambda Y(X)=\begin{cases}-\ln z_1 & \text{if } \hat{\mathbf{n}}\cdot\hat{\mathbf{y}}\ge 0 \text{ (upper half)},\\ -\ln z_2 & \text{if } \hat{\mathbf{n}}\cdot\hat{\mathbf{y}}\le 0 \text{ (lower half)},\end{cases} \tag{17}$$

which can, again, be expressed succinctly in the form of Eq. (1).

The problem of calculating the ECS has been reduced to the problem of finding the purely imaginary zeros of $\mathrm{Det}(\mathbf{1}-\mathbf{\Lambda})$. While it is straightforward to construct the matrix $\mathbf{\Lambda}$ for a given lattice, this is not necessary if the analytic form of the bulk free energy of the Ising system defined on either $\mathcal{L}$ or $\mathcal{L}^*$ is known. Using the FV method to evaluate Σ_{++} [cf. Eq. (7)], which is what the method was originally designed for,[10,11] one finds that the bulk free energy per unit cell of the model defined on $\mathcal{L}$ is given by

$$\beta f_b=\beta\varepsilon_0-\frac{1}{2}\int\int_{-\pi}^{\pi}\frac{dk_x dk_y}{(2\pi)^2}\ln\mathrm{Det}\{\mathbf{1}-\mathbf{\Lambda}_{\mathcal{L}^*}[k_x,k_y;\exp(-2K_{ij})]\}\ . \tag{18}$$

In Eq. (18), ε_0 is the ground-state energy per unit cell, the factor of $\frac{1}{2}$ comes from the fact that directed paths may be traversed in two directions, and the subscript $\mathcal{L}^*$ emphasizes that $\mathbf{\Lambda}$ describes a walk representing the interface on the dual lattice $\mathcal{L}^*$. Thus the ECS for the Ising system can simply be read off from the analytic form of the bulk free energy![31] This is a remarkable result because, naively at least, one would not expect the analytic form of the *bulk* free energy to contain complete information on the surface thermodynamics. The bulk free energy is normally given in terms of $\mathbf{\Lambda}_{\mathcal{L}}$ because the FV walker problem is traditionally formulated[10,11] in terms of high-T ($\tanh K$) graphs on the direct lattice $\mathcal{L}$. The corresponding form of the free energy is

$$\beta f_b=-\ln 2^{\ell}\prod\cosh K_{ij}-\frac{1}{2}\int\int_{-\pi}^{\pi}\frac{dk_x dk_y}{(2\pi)^2}\ln\mathrm{Det}\{\mathbf{1}-\mathbf{\Lambda}_{\mathcal{L}}[k_x,k_y;\tanh(K_{ij})]\}\ , \tag{19}$$

where ℓ is the number of sites per unit cell and the product is over all the bonds of the unit cell. As a direct consequence of the duality[21] between the systems on $\mathcal{L}$ and $\mathcal{L}^*$, Eq. (19) can simply be obtained from (18) by expressing $\exp(-2K_{ij})$ as $(1-\tanh K_{ij})/(1+\tanh K_{ij})$. Thus, equivalent expressions for the ECS of an Ising model on lattice $\mathcal{L}$ are

$$\begin{aligned}&\mathrm{Det}\{\mathbf{1}-\mathbf{\Lambda}_{\mathcal{L}^*}[k_x,k_y;\exp(-2K_{ij})]\}\ ,\\ &\mathrm{Det}\{\mathbf{1}-\mathbf{\Lambda}_{\mathcal{L}}[k_x,k_y;\tanh(K_{ij})]\}=0\ .\end{aligned} \tag{20}$$

On the other hand, if the bulk free energy of the dual system on $\mathcal{L}^*$ is known in terms of an integral over $\ln\mathrm{Det}\{\mathbf{1}-\mathbf{\Lambda}_{\mathcal{L}}[k_x,k_y;\exp(-2K_{ij}^*)]\}$ (low-T graphs) or $\ln\mathrm{Det}\{\mathbf{1}-\mathbf{\Lambda}_{\mathcal{L}^*}[k_x,k_y;\tanh(K_{ij}^*)]\}$ (high-T graphs), the expressions (20) [and, of course, also (19) and (18)] may be obtained via the duality transformation[21] $\exp(-2K_{ij}^*)\rightarrow\tanh K_{ij}$.

Once one has obtained the ECS from Eq. (1), one can use the inverse of the Wulff construction to determine the corresponding interfacial free energy per unit length $\gamma(\theta)$, or equivalently, the inverse of the (anisotropic) high-T correlation length $\xi^*(\theta+\pi/2)$ of the dual system [cf. Eq. (3)]. Given the ECS as $Y(X)$, the (2D) analytical form of the inverse Wulff construction is given by

$$\begin{aligned}\gamma(\theta)&=1/\xi^*(\theta+\pi/2)\\ &=\lambda X\sin\theta+\lambda Y\cos\theta,\quad \tan\theta\equiv-\frac{\partial Y}{\partial X}\ .\end{aligned} \tag{21}$$

It is generally not possible to obtain an analytic, closed-form expression for $\gamma(\theta)$ since this would generally involve finding the roots of polynomials of order higher than fourth.[32] Of course, Eq. (21) can always be implemented numerically to obtain $\gamma(\theta)$ to arbitrary accuracy.

Figures 2 and 3 show two examples of ECS's and corresponding interfacial free energies typical of ferromagnetic Ising models. These shapes display the following universal features of 2D Ising ECS's:[5] (1) The ECS becomes a circle as $T\rightarrow T_c^-$. For less symmetric lattices the ECS becomes an ellipse as $T\rightarrow T_c^-$ (see Fig. 9). This is a result of the fact that the lattice anisotropy is a marginal variable (in the renormalization-group sense). (2) The ECS, as obtained from Eq. (1) for fixed λ, vanishes in all directions linearly with T as $T\rightarrow T_c^-$. In Table I we give, for the convenience of the reader, the analytical form for the ECS of the Ising model defined on a number of commonly encountered lattices (Fig. 4). The results for the ECS of the square, triangular, and honeycomb lattices have been obtained previously[4,5] via the canonical formulation [see Eq. (3)] from the known correlation lengths of

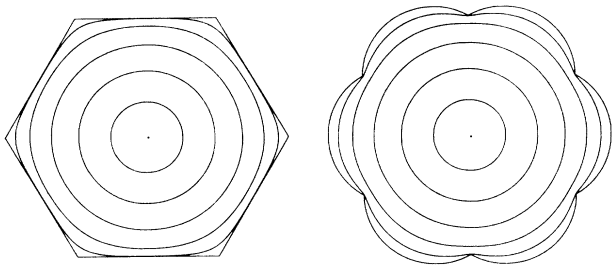

FIG. 2. ECS (left) and corresponding Wulff plot (right) of the diced lattice [Fig. 4(c)] for equal, ferromagnetic couplings. The Wulff plot [polar plot of the interfacial free energy per unit length, $\gamma(\theta)$] was obtained numerically from Eq. (21). Different curves correspond to different temperatures, spaced equally from 0 (polygon) to T_c (dot at center) at intervals of $T_c/6$.

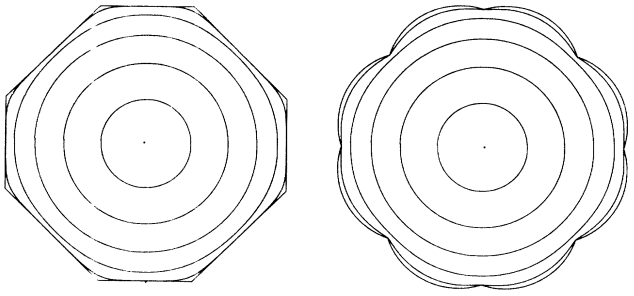

FIG. 3. Same as Fig. 2 for the 4-8 lattice with ferromagnetic couplings $K_1=K_2=K_3=K_4$ and $K_5=K_6$ as indicated in Fig. 4(d) with $K_1/K_5=\frac{1}{2}$. The horizontal and vertical faces at $T=0$ are associated with K_5; the diagonal ones with K_1.

these lattices.[33] We obtained the equations for the Kagomé and "Union Jack" lattices and their duals by explicit construction of the matrix $\mathbf{\Lambda}$. For the special cases $K_1=K_4$, $K_2=K_3$, and $K_5=K_6$ for the Kagomé lattice, and $K_1=K_2=K_3=K_4$ and $K_5=K_6$ for the "Union Jack" lattice, our result for $\mathrm{Det}(\mathbf{1}-\mathbf{\Lambda})$ reduces to that which can be read off from the bulk free energy as obtained by Kano and Naya[34] and by Vaks, Larken, and Ovchinnikov,[35] respectively.

In the derivation above, we had ferromagnetic Ising models in mind. However, the properties of the model crucial for our derivation are satisfied for a wider class of models. Hurst and Green[36] have shown that the FV method is equivalent to the Pfaffian[12] method, which can be used to solve any model which can be written as a free fermion field theory, i.e., a field theory which is quadratic in fermionic operators. The factors of (-1) which appear in the FV method are directly related to the (-1)'s of fermion anticommutators, and the uncoupling of directed graphs, necessary for the FV method to work, is precisely

TABLE I. Analytic expressions for the ECS's of the lattices indicated. The labeling of the interactions and the basis vectors **a** and **b** are defined in Fig. 4.

Examples of exact equilibrium crystal shapes

$$A-B\cosh(\beta\lambda\mathbf{a}\cdot\mathbf{Y})-C\cosh(\beta\lambda\mathbf{b}\cdot\mathbf{Y})-D\cosh[\beta\lambda(\mathbf{a}+\mathbf{b})\cdot\mathbf{Y}]-E\cosh[\beta\lambda(\mathbf{a}-\mathbf{b})\cdot\mathbf{Y}]=0$$
$$\mathbf{Y}\equiv(-Y,X);\quad c_i\equiv\cosh(2K_i),\quad s_i\equiv\sinh(2K_i)$$

Rectangular	Triangular	Honeycomb
$A=c_1c_2$	$A=c_1c_2c_3+s_1s_2s_3$	$A=c_1c_2c_3+1$
$B=s_1$	$B=s_1$	$B=s_2s_3$
$C=s_2$	$C=s_2$	$C=s_1s_3$
$D=0$	$D=s_3$	$D=s_1s_2$
$E=0$	$E=0$	$E=0$

Kagomé	Diced
$A=(c_1c_3c_5+s_1s_3s_5)(s_2s_4s_6+c_2c_4c_6)+c_1c_4+c_2c_3+c_5c_6$	$A=c_5c_6(c_1c_2c_3c_4+s_1s_2s_3s_4)+s_5s_6(c_1c_4s_2s_3+c_2c_3s_1s_4)+c_1c_3c_5+c_2c_4c_6+1$
$B=c_4s_1s_2s_6+c_1s_3s_4s_5+s_1s_4(c_2c_6+c_3c_5)$	$B=s_2s_6(c_1+c_3c_5)+s_3s_5(c_4+c_2c_6)$
$C=c_2s_3s_4s_6+c_3s_1s_2s_5+s_2s_3(c_1c_5+c_4c_6)$	$C=s_4s_6(c_3+c_1c_5)+s_1s_5(c_2+c_4c_6)$
$D=c_5s_1s_3s_6+c_6s_2s_4s_5+s_5s_6(c_1c_3+c_2c_4)$	$D=s_2s_4(c_5+c_1c_3)+s_1s_3(c_6+c_2c_4)$
$E=0$	$E=0$

"Union Jack"	4-8
$A=c_5c_6(c_1c_2c_3c_4+s_1s_2s_3s_4+1)+s_5c_6(c_1c_2s_3s_4+s_1s_2c_3c_4)+c_5s_6(c_1c_4s_2s_3+s_1s_4c_2c_3)+s_5s_6(c_1c_3s_2s_4+s_1s_3c_2c_4)$	$A=c_5c_6(c_1c_2c_3c_4+s_1s_2s_3s_4)+c_5(c_1c_4+c_2c_3)+c_6(c_1c_2+c_3c_4)+c_1c_3+c_2c_4+c_5c_6$
$B=s_5(c_1c_2+c_3c_4)+c_5(s_1s_2+s_3s_4)$	$B=s_1s_2s_6(c_3c_4+c_5)+s_3s_4s_6(c_1c_2+c_5)$
$C=s_6(c_1c_4+c_2c_3)+c_6(s_1s_4+s_2s_3)$	$C=s_2s_3s_5(c_1c_4+c_6)+s_1s_4s_5(c_2c_3+c_6)$
$D=s_2s_4$	$D=s_1s_3s_5s_6$
$E=s_1s_3$	$E=s_2s_4s_5s_6$

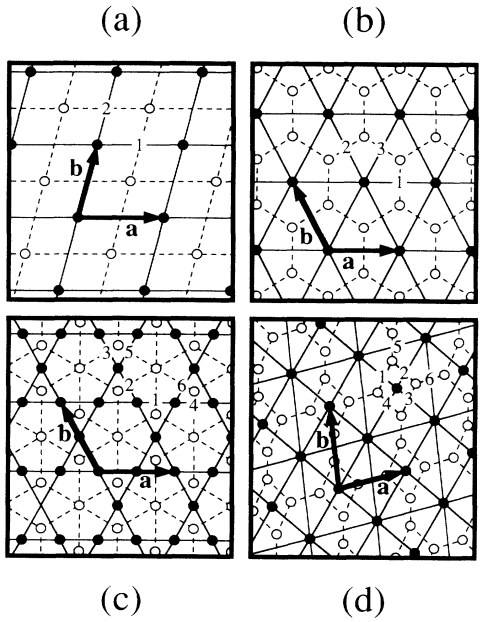

FIG. 4. Lattices of Table I in duality pairs: (a) rectangular lattice (self-dual), (b) triangular and honeycomb lattices, (c) Kagomé lattice (solid) and diced lattice (dashed), and (d) "Union Jack" lattice (solid) and 4-8 lattice (dashed). The labeling of bonds and the definition of basis vectors correspond to those used in Table I. The position of sites within the unit cell, defined by the basis vectors **a** and **b**, is arbitrary. In the figure these sites were placed at symmetric positions for aesthetic reasons.

due to the field theory being free. The upshot of this equivalence is that we know the ECS for *any* model solvable by the Pfaffian or FV method, in the form of the poles of the determinant of the free-fermion propagator [Eq. (1)], provided that the FV walk can be identified with an interface between coexisting phases.

III. EXAMPLE OF NON-ISING FREE-FERMION CRYSTAL SHAPES: THE MODIFIED KDP MODEL

We will now demonstrate the validity of Eq. (1) for the modified KDP model,[16,17] a non-Ising free-fermion model. To be precise, we shall show that the purely imaginary poles of the determinant of the free-fermion propagator of the modified KDP model will correctly give the ECS of the dual model. The dual model turns out to be the limit of an antiferromagnetic Ising model on a triangular lattice as the interactions become infinite. The resulting ECS's have sharp corners for any $T < T_c$. The interface configurations of this model are extremely simple so that the solutions obtained from (1) can be confirmed via an independent elementary calculation. Historically, the 2D KDP model[37] was proposed as a model having the characteristics of the ferroelectric potassium dihydrogen phosphate (KH_2PO_4). The modified KDP model is a special (more simple) version of the KDP model in which a certain configuration has been suppressed but which still has many of the essential features of the full KDP model.[38]

The modified KDP model is a special case of the eight-vertex model.[13–15] The square-lattice eight-vertex model is defined by eight types of vertices, as shown in Fig. 5, which must be placed on the vertices of a square lattice, such that arrows from different vertices sharing the same bond point in the same direction. Each vertex carries a Boltzmann weight $\omega_i = \exp(-\beta e_i)$, $i = 1, 2, \ldots, 8$. When these weights satisfy the so-called free-fermion condition[36,38]

$$\omega_1\omega_2 + \omega_3\omega_4 = \omega_5\omega_6 + \omega_7\omega_8 , \tag{22}$$

the square-lattice eight-vertex model is solvable by the Pfaffian method[12] and, therefore, by the FV method. Equation (22) is satisfied by any eight-vertex model at one particular temperature. When the weights ω_i are chosen such that (22) is satisfied at all temperatures, the model is known as *the* free-fermion model.[38] Depending on the particular choices for the ω_i, the free-fermion model can be shown to be either trivial (decoupled 1D chains), equivalent to the Ising model on a triangular lattice or, in a certain limiting case (see below), equivalent to the modified KDP model, which in turn turns out to be equivalent to the close-packed dimer model on a hexagonal lattice.[17]

We shall first show how the free-fermion model is solved by the FV method. Specializing to the modified KDP model, we will then identify the corresponding walk with microscopic interface configurations separating coexisting phases of the dual model. The FV method was used by Ryazanov[39] to calculate the bulk free energy of the modified KDP model in zero (electric) field. It is straightforward to generalize this particular solution to

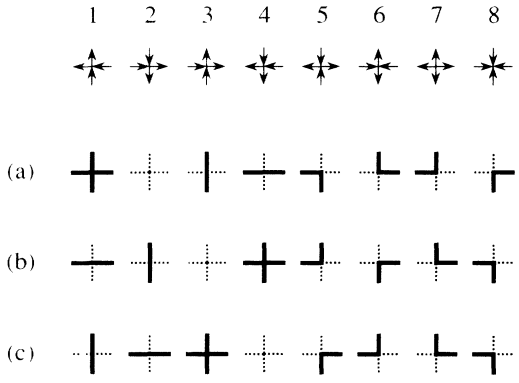

FIG. 5. Eight vertex configurations of the eight-vertex model. As an alternative to representing vertex configurations by arrows, one can represent them by "bond arrangements." These bond arrangements are constructed from the arrow representation by first choosing (arbitrarily) a vertex which corresponds to no bonds (no bold lines), the basis. Other bond configurations are then constructed from the basis by drawing a bond for every arrow pointing in a direction opposite to that of the corresponding arrow of the basis vertex. (a), (b), and (c) show three of the eight possible bond arrangements based on the vertices 2, 3, and 4, respectively.

the general free-fermion model. To identify the "random" walker counting problem, it is convenient to represent the vertices as "bond arrangements".[38] There are eight possible bond arrangements, three of which are shown in Fig. 5. In the absence of macroscopic interfaces, allowed vertex configurations correspond to closed loops of bonds, and calculating the partition function reduces to the problem of counting all possible loop configurations. Since the loop counting is on a square lattice, the appropriate walking matrix Λ is 4×4 and schematically given by

$$\Lambda = \begin{pmatrix} \cdots & \cdots & 0 & \cdots \\ \cdots & \cdots & \cdots & 0 \\ 0 & \cdots & \cdots & \cdots \\ \cdots & 0 & \cdots & \cdots \end{pmatrix} . \tag{23}$$

This matrix involves only six vertices. The remaining two, corresponding to no bonds and intersecting bonds, are automatically taken into account correctly by virtue of the free-fermion condition (22). With the choice of bond arrangement (a) of Fig. 5, Λ becomes [cf. Eq. (11)]

$$\Lambda = \frac{1}{\omega_2} \begin{pmatrix} \omega_3 e_{-y} & \alpha^{-1}\omega_6 e_{-y} & 0 & \alpha\omega_7 e_{-y} \\ \alpha\omega_5 e_x & \omega_4 e_x & \alpha^{-1}\omega_7 e_x & 0 \\ 0 & \alpha\omega_8 e_y & \omega_3 e_y & \alpha^{-1}\omega_5 e_y \\ \alpha^{-1}\omega_8 e_{-x} & 0 & \alpha\omega_6 e_{-x} & \omega_4 e_{-x} \end{pmatrix} , \tag{24}$$

where vertex energy is measured with respect to vertex 2 (Fig. 5), which corresponds to no bonds, and $\alpha \equiv e^{-i\pi/4}$, $e_{\pm x} \equiv e^{ik_{\pm x}}$, and $e_{\pm y} \equiv e^{ik_{\pm y}}$. Equation (24) yields the same bulk free energy as obtained by Hurst and Green[36] and by Fan and Wu[13,14] via other methods. We find [making use of (22)]

$$\begin{aligned} \mathrm{Det}(\mathbf{1}-\Lambda) = {} & a + 2b\cos k_x + 2c\cos k_y \\ & + 2f\cos(k_x - k_y) + 2g\cos(k_x + k_y) , \end{aligned} \tag{25}$$

where $a = \omega_1^2+\omega_2^2+\omega_3^2+\omega_4^2$, $b = \omega_1\omega_3 - \omega_2\omega_4$, $c = \omega_1\omega_4 - \omega_2\omega_3$, $f = \omega_3\omega_4 - \omega_5\omega_6$, and $g = \omega_3\omega_4 - \omega_7\omega_8$. The bulk free energy of the free-fermion model is independent of the choice of "bond arrangement," because the integral of $\ln \mathrm{Det}(\mathbf{1}-\Lambda)$ is invariant under change of arrangement. However, crystal shapes are obtained from $\mathrm{Det}(\mathbf{1}-\Lambda)$ itself, which *does* depend on the choice of "bond arrangement." As we shall see, it is necessary to identify the coexisting phases for which we wish to calculate the ECS, before the correct bond arrangement can be chosen.

We define the modified KDP model as the limit of the free-fermion eight-vertex model

$$\begin{aligned} & e_1,\ e_2 = h + v,\ e_3 = \varepsilon - h + v,\ e_4 = \varepsilon + h - v , \\ & e_5 = e_6 = \varepsilon,\ e_7 = \frac{e_1}{2} + h,\ e_8 = \frac{e_1}{2} + v , \end{aligned} \tag{26}$$

in the limit $e_1 \to \infty$. The variables h and v correspond to horizontal and vertical electric fields in the original KDP model.[37] In the limit $e_1 = \infty$, analysis of the bulk free energy[14] shows that this model has a second-order phase transition which is *not* of the Ising type. As $T \to T_c^+$, the specific heat has a $(T-T_c)^{-1/2}$ divergence instead of the $\ln|T-T_c|$ divergence of the Ising model. The critical temperature is given by the condition $\omega_2+\omega_3+\omega_4 = 2\max(\omega_2,\omega_3,\omega_4)$, which divides the h-v plane into three distinct regions: $h < \varepsilon/2$ and $v < \varepsilon/2$ define the region $\mathcal{R}_2$, where ω_2 is largest; $h > \varepsilon/2$ and $v < h$ define the region $\mathcal{R}_3$, where ω_3 is largest; $h < v$ and $v > \varepsilon/2$ define the region $\mathcal{R}_4$, where ω_4 is largest.

The identification of the walk described by the matrix Λ of Eq. (23) with a microscopic interface configuration separating coexisting phases is most easily accomplished in the familiar language of the Ising model by making use of the following duality:[13,38] Any eight-vertex model on a square lattice is dual to an Ising model on the dual lattice with four-spin interactions and (crossing-bond) next-nearest-neighbor interactions. In terms of this equivalent Ising model, the free-fermion condition is the condition that the four-spin interaction and one of the next-nearest-neighbor interactions be zero. The free-fermion eight-vertex model (26) is, therefore, dual to an "Ising" model on a triangular lattice (at least for finite e_1), which is calculated to have interaction energies[38]

$$\begin{aligned} & J_1 = \tfrac{1}{4}(-e_1 + 3h - v) , \\ & J_2 = \tfrac{1}{4}(-e_1 + 3v - h) , \\ & J_3 = \tfrac{1}{4}(-e_1 + 2\varepsilon - h - v) , \end{aligned} \tag{27}$$

where $J_i > 0$ corresponds to ferromagnetic coupling. In terms of these Ising energies, the vertex weights become[38]

$$\begin{aligned} & e_1 + J_0 = -J_1 - J_2 - J_3,\ e_2 + J_0 = J_1 + J_2 - J_3 , \\ & e_3 + J_0 = -J_1 + J_2 + J_3,\ e_4 + J_0 = J_1 - J_2 + J_3 , \\ & e_5 + J_0 = e_6 + J_0 = J_3,\ e_7 + J_0 = e_8 + J_0 = -J_3 , \end{aligned} \tag{28}$$

where the overall constant $J_0 = \frac{1}{4}(-e_1 - 2\varepsilon - h - v)$.

Since we are interested in the limit $e_1 \to \infty$, we focus on the completely antiferromagnetic sector of the model (27), where e_1 is finite, but large enough to make all Ising couplings negative. This sector is defined for $e_1 > \varepsilon > 0$ and consists of a triangular region in the h-v plane (see Fig. 6). Within this triangular region, we identify the same three regions of the h-v plane as those for the modified KDP model. The interior of each region is characterized by one bond being weaker than the others. The weakest bond in $\mathcal{R}_2$, $\mathcal{R}_3$, and $\mathcal{R}_4$ is J_3, J_1, and J_2, respectively. On the boundaries where regions meet, two bond energies are equal and weaker than the third, except at the point $h = v = \varepsilon/2$, where all couplings are equal. We can now identify the nature of the phases in the interior of each region and on the boundaries. In the interior of each region is a 2×1 phase which consists of rows of predominantly aligned spins. The rows are along the direction of the weakest bond, and the sign of the alignment of the spins alternates from row to row. Within

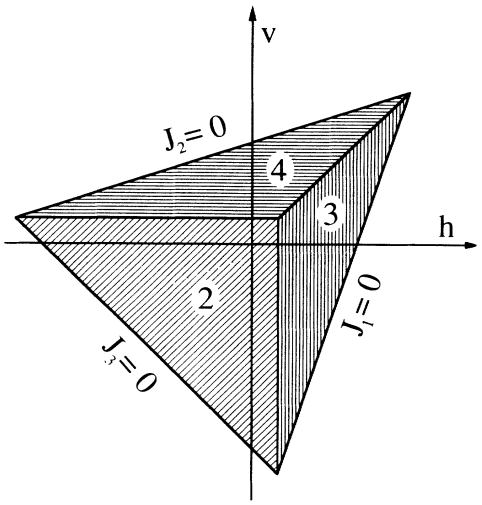

FIG. 6. Antiferromagnetic sector of the free-fermion model defined by the vertex weights of Eq. (26), in the h-v plane of horizontal and vertical (electric) fields. In regions 2, 3, and 4, the ground state of the model is given by vertices 2, 3, and 4. In terms of the equivalent Ising couplings, the regions, 2, 3, and 4 are characterized by 2×1 phases aligned along bonds J_3, J_1, and J_2, respectively. As $e_1\to\infty$, the modified KDP model is approached, and the boundaries of the antiferromagnetic sector are pushed to infinity.

each region, the 2×1 phase has two degenerate realizations, related by an overall change of sign, which constitute the two phases which can coexist in zero magnetic field below T_c (see Fig. 7). The ECS is thus well defined in the interior of each region, $\mathcal{R}_2$, $\mathcal{R}_3$, and $\mathcal{R}_4$, and corresponds to the shape of a macroscopic inclusion of an appropriately oriented 2×1 phase coexisting with a 2×1 phase of the same orientation but opposite overall sign.[40] On the boundaries where regions meet, the ground state is macroscopically degenerate and there is no ordered phase at any temperature.

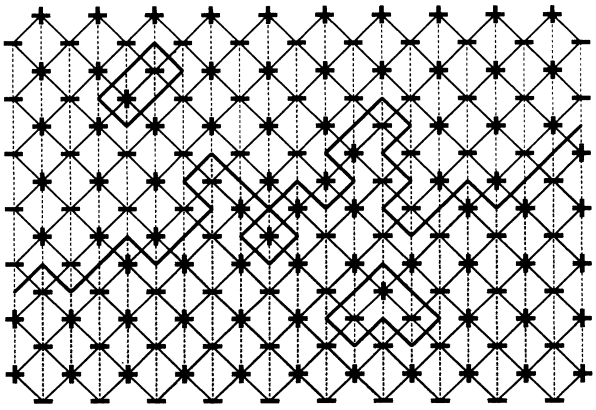

FIG. 7. An interface between two degenerate 2×1 phases of the antiferromagnetic triangular Ising model. The dashed bond is weaker than the others so that the ground state corresponds to spins aligned in rows along the dashed lines.

The walk of the FV method can now easily be identified as a microscopic interface configuration: The bold lines of bond arrangements correspond to composite elementary interfaces on the hexagonal lattice dual to the triangular Ising system (27), as shown in Fig. 8. Depending on which bond arrangement is chosen, these interface configurations carry different vertex weights e_i (Fig. 5). To interpret these energies as the energies needed to create the composite interfaces of Fig. 8 from the ground-state configuration, we must first identify the ground-state energy per vertex. It follows from Eqs. (28) that the energy for the 2×1 ground state of $\mathcal{R}_2$, $\mathcal{R}_3$, and $\mathcal{R}_4$ corresponds to the energy of vertex 2, 3, and 4, respectively. Subtracting the ground-state energies, one can now easily identify the vertex energies of bond arrangements (a), (b), and (c) as precisely the energies needed to create the corresponding broken bonds *per vertex* from the 2×1-phase ground states of regions $\mathcal{R}_2$, $\mathcal{R}_3$, and $\mathcal{R}_4$, respectively (see Figs. 5 and 8). Different bond arrangements result in different weights for the entries of the matrix $\mathbf{\Lambda}$ [cf. Eq. (23)], which leads to different functions $\mathrm{Det}(\mathbf{1}-\mathbf{\Lambda})$. It is now clear that the matrix $\mathbf{\Lambda}$ based on bond arrangement (a), with vertex 2 describing the ground state, can describe elementary interfaces of the antiferromagnetic triangular Ising model only in $\mathcal{R}_2$. To obtain the ECS in $\mathcal{R}_3$ and $\mathcal{R}_4$, $\mathbf{\Lambda}$ must be based on bond arrangements (b) and (c), respectively. $\mathrm{Det}(\mathbf{1}-\mathbf{\Lambda})$ for $\mathcal{R}_3$ is obtained from Eq. (25) by making the substitutions $(\mathrm{b,f,g})\to(-\mathrm{b},-\mathrm{f},-\mathrm{g})$, and for $\mathcal{R}_4$, by making the substitutions $(\mathrm{c,f,g})\to(-\mathrm{c},-\mathrm{f},-\mathrm{g})$.

Before we take the limit $e_1\to\infty$, let us look at the kind of shapes one obtains with bond arrangement (a) for finite e_1. In Fig. 9 we show the shapes obtained from Eq. (25) with the vertex weights (26) at $h=v=0$ for increasing values of e_1. For $e_1/\varepsilon<2$, $J_3>0$, and we are outside the antiferromagnetic sector. The signs of J_1 and J_2 may be reversed by symmetry, so that, for these couplings, the model is equivalent to the triangular ferromagnetic Ising model. The value $e_1/\varepsilon=2$ corresponds to sitting on the boundary of the antiferromagnetic sector with $J_3=0$.

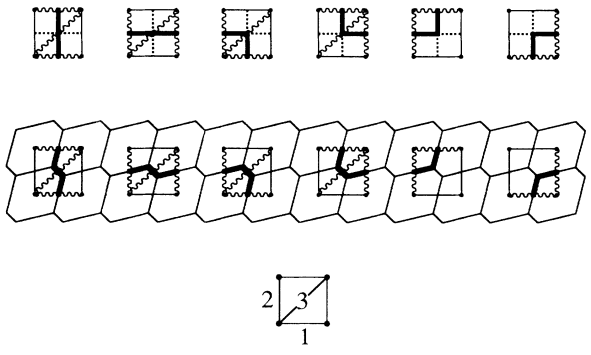

FIG. 8. One-to-one correspondence between vertex configurations of the eight-vertex model and composite elementary interfaces on the hexagonal lattice. The wavy lines correspond to broken bonds of the triangular dual lattice which has interactions J_1, J_2, and J_3 as shown.

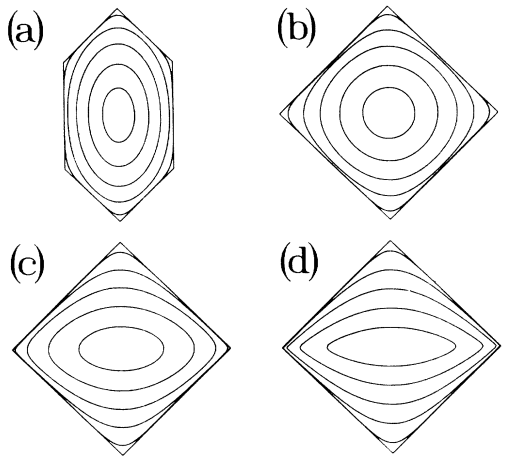

FIG. 9. Equilibrium crystal shapes of the free-fermion model defined by the vertex weights of Eq. (26) at $h=v=0$ and for various values of e_1/ε: (a) $e_1/\varepsilon=1$, (b) $e_1/\varepsilon=2$, (c) $e_1/\varepsilon=4$, and (d) $e_1/\varepsilon=8$. In each case, the ECS has been plotted at temperatures equally spaced from 0 to T_c at intervals of $T_c/6$. The lattice of the model was chosen to have the same basis and orientation as shown in Fig. 7, with the weakest bond in the horizontal direction. Shapes (a) and (b) are the ECS's of a macroscopic inclusion of "up" phase in a sea of "down" phase for the ferromagnetic triangular and square Ising models, respectively. Shapes (c) and (d) are the ECS's of a macroscopic inclusion of 2×1 phase in another of opposite (staggered) magnetization (see Fig. 7). With increasing value of e_1/ε, the modified KDP model ($e_1/\varepsilon=\infty$) is approached and the corners pointing in the direction perpendicular to the weakest bond become increasingly sharp.

This is equivalent to an antiferromagnetic rectangular Ising model, which (again, by symmetry) is identical to a ferromagnetic rectangular Ising model. For $e_1/\varepsilon>2$, we are in region $\mathcal{R}_2$ of the antiferromagnetic sector of the triangular Ising model and the coexisting phases are 2×1 phases aligned along the direction of bond J_3. Note that, with increasing e_1, the corners "pointing" in the direction perpendicular to the weakest bond J_3 become increasingly sharp.

Setting $e_1=\infty$ in Eqs. (27) shows that the modified KDP model is dual to an antiferromagnetic "Ising" model on a triangular lattice with infinite interactions differing from each other by a finite amount. The infiniteness of these interactions severely restricts the possible interface configurations, because any interface must make maximal use of the weakest bonds. Thus, the walker generating the interface performs a very simple walk: After a step along the easiest elementary interface (along the bond dual to the weakest bond of the triangular lattice), he can either step to the right or to the left. Next, he is forced to again take a step along the easiest elementary interface, and so on. The simplicity of this walk is reflected in the structure of the matrix $\mathbf{\Lambda}$, which becomes the direct sum of two 2×2 matrices, when $\omega_1=\omega_7=\omega_8=0$. The determinant of the propagator factors, therefore, into two simple expressions. One describes the upper half of the crystal shape; the other, the lower. For $\mathcal{R}_2$ one finds for the ECS the simple expression

$$\omega_3 e^{-\beta\lambda X}+\omega_4 e^{-\beta\lambda Y}-\omega_2=0 \text{ and } (X,Y)\rightarrow(-X,-Y) \quad (h,v)\in\mathcal{R}_2 . \tag{29}$$

The corresponding equations for $\mathcal{R}_3$ and $\mathcal{R}_4$ are obtained from Eq. (29) by making the substitutions $\omega_4\rightarrow-\omega_4$ and $\omega_3\rightarrow-\omega_3$, respectively. Note that the pair of functions (29) (and the corresponding ones in $\mathcal{R}_3$ and $\mathcal{R}_4$) describe curves of infinite extent and that the ECS is to be interpreted as the convex region enclosed by the two functions for $T<T_c$. Where the pair of curves intersect, the ECS has a sharp corner which moves toward the origin like $(T_c-T)^{1/2}$, as $T\rightarrow T_c^-$. In all other directions the ECS vanishes linearly with T, as $T\rightarrow T_c^-$. The sharp corners and the fact that the crystal shape appears to be analytically continued beyond the convex region[41] are unusual features of the ECS and are a direct result of the infiniteness of the interactions. To gain further insight into the physical origin of these features, we make use of the simplicity of the interface configurations to calculate—in a very direct and elementary manner—the interfacial free energy and the crystal shape.

Consider the infinite-interaction "Ising" model dual to the KDP model on an arbitrary triangular lattice, so that the corresponding FV walk takes place on an arbitrary hexagonal lattice. Let the easiest steps on the hexagonal lattice be denoted by $\mathbf{d}_w$ and $-\mathbf{d}_w$ and denote the steps to the right and left of $\mathbf{d}_w$ by $\mathbf{d}_r$ and $\mathbf{d}_\ell$, respectively. Because of the infiniteness of the interactions, the walker actually performs a walk on a rectangular lattice with the composite steps $\pm\mathbf{d}_1$ and $\pm\mathbf{d}_2$, where $\mathbf{d}_1=\mathbf{d}_w+\mathbf{d}_r$ and $\mathbf{d}_2=\mathbf{d}_w+\mathbf{d}_\ell$. Since a step $\pm\mathbf{d}_1$ or $\pm\mathbf{d}_2$ of given sign must be followed by a step of the same sign, the only interfaces available to the (say) upper half of the ECS must have tangent vectors which lie between $\mathbf{d}_1$ and $\mathbf{d}_2$ (see Fig. 10). It is precisely the absence of other interface orientations which causes the sharp corners of the ECS. The zero-temperature character of the infinite interactions manifests itself in the fact that the entropy of a walk from the origin to the point $\mathbf{R}=n\mathbf{d}_1+m\mathbf{d}_2$ $(m,n>0)$ is simply given by the zero-temperature entropy, $\ln[(n+m)!/(n!m!)]$, at all temperatures. If E_1 and E_2 denote the costs in energy of taking steps $\pm\mathbf{d}_1$ and $\pm\mathbf{d}_2$, we can immediately write down the corresponding free energy per unit length, $\gamma(\theta)$, as

$$\gamma(\theta)=\tilde{n}E_1+\tilde{m}E_2 -\frac{1}{\beta}[(\tilde{n}+\tilde{m})\ln(\tilde{n}+\tilde{m})-\tilde{n}\ln\tilde{n}-\tilde{m}\ln\tilde{m}] \quad \theta\in[0,\theta_{\max}]\cup[\pi,\pi+\theta_{\max}] , \tag{30}$$

where $\tilde{n}\equiv n/R$, $\tilde{m}\equiv m/R$, θ is measured clockwise from the $\hat{\mathbf{z}}\times\mathbf{d}_2$ direction, and $\cos\theta_{\max}=\mathbf{d}_1\cdot\mathbf{d}_2/(d_1d_2)$. Explicitly, we find $\tilde{m}=(\cos\theta-\sin\theta\cot\theta_{\max})/d_2$ and $\tilde{n}=\sin\theta/(d_1\sin\theta_{\max})$. Performing the Wulff construction for each of the two branches of $\gamma(\theta)$ *separately* (i.e., separately for $\theta\in[0,\theta_{\max}]$ and for $\theta\in[\pi,\pi+\theta_{\max}]$), one finds

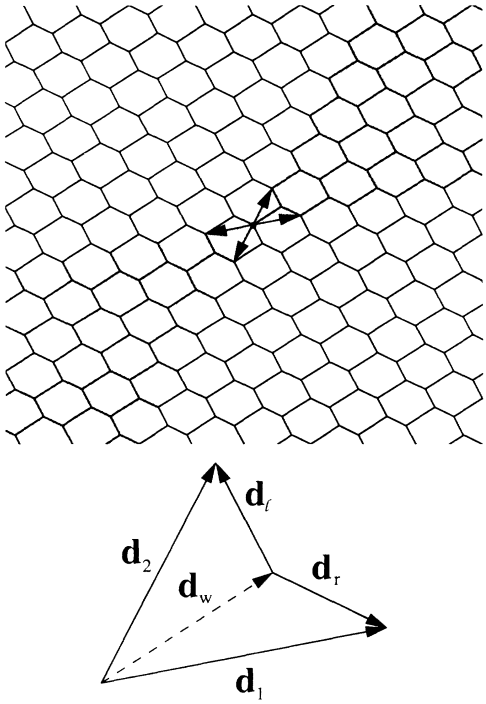

FIG. 10. Feynman-Vdovichenko walker for the modified KDP model performs a very simple walk on the honeycomb lattice: The infiniteness of the interactions forces the walker to make maximal use of the lowest-energy step, which we take to be $\pm\mathbf{d}_w$. Every step $\mathbf{d}_w$ is followed by a step $\mathbf{d}_r$ or $\mathbf{d}_l$ which must be followed again by a step $\mathbf{d}_w$, and so on. Thus the walk takes place effectively on a square lattice with the composite steps $\pm\mathbf{d}_1$ and $\pm\mathbf{d}_2$. Since every composite step must be followed by a composite step of the same sign, only the shaded regions are accessible to a walker starting out at a given lattice site. The fact that directions outside the shaded regions are forbidden is what causes the sharp corners of the ECS of the modified KDP model and gaps in the corresponding Wulff plot.

that the envelope of the Wulff lines for each branch produces an infinitely extended curve. The pair of curves thus obtained is given by

$$e^{(\beta/2)[E_1+E_2+(\mathbf{d}_1+\mathbf{d}_2)\cdot\mathbf{Y}]} = 2\cosh\left[\frac{\beta}{2}[E_1-E_2+(\mathbf{d}_1-\mathbf{d}_2)\cdot\mathbf{Y}]\right] \quad (31)$$

and

$$(\mathbf{d}_1,\mathbf{d}_2)\rightarrow(-\mathbf{d}_1,-\mathbf{d}_2)\ ,$$

where $\mathbf{Y}\equiv(-Y,X)$. Equation (29) and the corresponding equations in $\mathcal{R}_3$ and $\mathcal{R}_4$ are special cases of (31) corresponding to $(\mathbf{d}_1,\mathbf{d}_2)$ equal to $(-\hat{\mathbf{y}},\hat{\mathbf{x}})$, $(\hat{\mathbf{x}},\hat{\mathbf{x}}+\hat{\mathbf{y}})$, and $(\hat{\mathbf{x}}+\hat{\mathbf{y}},\hat{\mathbf{y}})$, respectively, and are just rotations and linear distortions of one another. The interior envelope of *all* Wulff planes is just the convex region enclosed by both curves and results in a ECS with sharp corners (see Fig. 11).[42]

For completeness we mention that the ECS (31) can be calculated very simply by mapping the interface

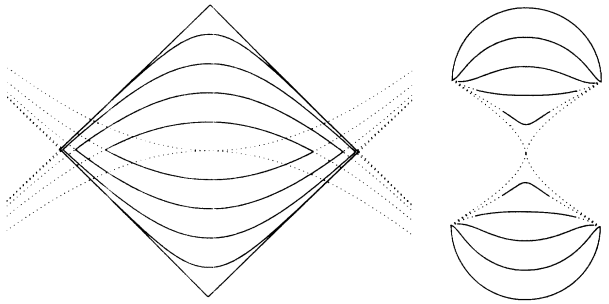

FIG. 11. ECS of the modified KDP model (solid lines, left) and the corresponding Wulff plot (right) for $h=v=0$. The curves have been plotted at temperatures equally spaced from 0 to T_c at intervals of $T_c/5$. The dual lattice for the model has been chosen to have the basis and orientation shown in Fig. 7. At finite T, those orientations corresponding to the dashed lines do not contribute to the ECS and are, therefore, thermodynamically unstable (Ref. 43).

configurations of the modified KDP model onto a one-dimensional Ising model. This is very similar in spirit to the work of Shi and Wortis.[43] Each step of the walk can be in two "states," along either $\mathbf{d}_1$ or $\mathbf{d}_2$ [$(\downarrow)$ or $(\uparrow)$]. Because successive steps do not interact in the case of the modified KDP model, the 1D Ising model reduces to a zero-dimensional model consisting of a single "spin." By rearranging Eq. (5), one can express the ECS as

$$1=\mathrm{Tr}\exp\left[-\frac{\beta}{2}[(E_\downarrow+E_\uparrow)+(E_\downarrow-E_\uparrow)\sigma]\right],\quad \sigma=\pm1\ , \quad (32)$$

with

$$E_\downarrow=E_1+\mathbf{d}_1\cdot\mathbf{Y},\quad E_\uparrow=E_2+\mathbf{d}_2\cdot\mathbf{Y}\ , \quad (33)$$

which immediately yields Eq. (31) for the general ECS.

IV. CONCLUSION

We have found a general, exact solution for the ECS's of free-fermion models. This solution was derived in a "grand canonical" ensemble of interface orientations and made use of an exact mapping of the interface onto a Feynman-Vdovichenko walker. This mapping is possible, because free-fermion models allow bulk fluctuations to be effectively uncoupled from interface fluctuations via the inclusion of appropriate minus signs into the Boltzmann weights. The ECS of free-fermion models turns out to be remarkably simple: The ECS is given by the locus of purely imaginary poles of the determinant of the lattice-path propagator. Because the bulk free energy of these models is usually expressed as an integral over the logarithm of this determinant, the ECS can simply be read off from the analytic form of the bulk free energy.

2D Ising models without crossing bonds are free-fermion models. Prior to the work of Ref. 9 and the present paper, the only known exact 2D Ising ECS's were those of the rectangular, triangular, and honeycomb lat-

tices. New Ising results are easily obtained either by explicitly constructing the FV matrix or by reading off $\mathrm{Det}(\mathbf{1}-\mathbf{\Lambda})$ from the analytic form of the bulk free energy (if already known). As examples of new solutions, we give in Table I the ECS's of the Kagomé and "Union Jack" lattices and their duals, the diced and 4–8 lattices, respectively (see also Figs. 2 and 3).

From a study of the free-fermion case of the eight-vertex model (*the* free-fermion model), we demonstrated that one must generally be careful in reading off the ECS from the bulk free energy. While many different forms of the FV matrix give the same bulk free energy, these different matrices represent interfaces between different coexisting phases and, therefore, result in different ECS's. The modified KDP model is a special case of the free-fermion model which is not in the Ising universality class. The ECS of the modified KDP model is the limit of the ECS defined for coexisting 2×1 phases of a triangular antiferromagnet in the limit of infinite interactions differing by a finite amount. The ECS of the modified KDP model is lenticular and has, as a consequence of the infinite interactions, sharp corners. The infinite interactions greatly simplify the interface configurations possible and allow elementary calculation of the ECS, which confirms the result obtained from the general solution.

ACKNOWLEDGMENTS

It is a pleasure to thank M. Wortis for his patience and encouragement during many very helpful discussions. During the course of various parts of this work, I have also benefitted from conversations with M. Plischke, M. Rao, and R. K. P. Zia. Support from Simon Fraser University is gratefully acknowledged.

*Present address: Laboratory of Atomic and Solid State Physics, Cornell University, Ithaca, New York 14853-2501.

[1]G. Wulff, Z. Kristallogr. Mineral. **34**, 449 (1901); C. Herring, Phys. Rev. **82**, 87 (1951).

[2]For recent reviews, see H. van Beijeren and I. Nolden, in *Topics in Current Physics*, edited by W. Schommers and P. von Blanckenhagen (Springer-Verlag, Berlin, 1987), Vol. 43, pp. 259–300; M. Wortis, in *Chemistry and Physics of Solid Surfaces*, edited by R. Vanselow (Springer-Verlag, Berlin, 1988), Vol. VII, pp. 367–405; for a more mathematical point of view, see, for example, R. Kotecký, in *Proceedings of the Ninth International Congress of Mathematical Physics*, edited by B. Simon, I. M. Davies, and A. Truman (Hilger, Bristol, England, 1988).

[3]See, for example, the review by H. J. Leamy, G. H. Gilmer, and K. A. Jackson, in *Surface Physics of Crystalline Materials*, edited by J. M. Blakely (Academic, New York, 1975), p. 169, and references therein.

[4]C. Rottman and M. Wortis, Phys. Rev. B **24**, 6274 (1981); J. E. Avron, H. van Beijeren, L. S. Schulman, and R. K. P. Zia, J. Phys. A **15**, L81 (1982); R. K. P. Zia and J. E. Avron, Phys. Rev. B **25**, 2042 (1982).

[5]R. K. P. Zia, J. Stat. Phys. **45**, 801 (1986).

[6]The interfacial free energies for the symmetry directions of the rectangular, triangular, and honeycomb lattices were first published by M. E. Fisher and A. E. Ferdinand, Phys. Rev. Lett. **19**, 169 (1967).

[7]N. Akutsu and Y. Akutsu, J. Phys. Soc. Jpn. **56**, 2248 (1987).

[8]M. Holzer and M. Wortis, Phys. Rev. B **40**, 11 044 (1989).

[9]M. Holzer, Phys. Rev. Lett. **64**, 653 (1990). Via a very similar calculation, Akutsu and Akutsu also arrived at this solution: Y. Akutsu and N. Akutsu, Phys. Rev. Lett. **64**, 1189 (1990).

[10]N. V. Vdovichenko, Zh. Eksp. Teor. Fiz. **47**, 715 (1964) [Sov. Phys.—JETP **20**, 477 (1965)]; see also L. D. Landau and E. M. Lifshitz, *Statistical Physics*, 2nd ed. (Pergamon, Oxford, 1968), pp. 447–454; T. Morita, J. Phys. A **19**, 1197 (1986).

[11]Feynman's solution for the bulk free energy of the Ising model predates Vdovichenko's [see S. Sherman, J. Math. Phys. **1**, 202 (1960)], but was apparently not published until 1972. His solution is only slightly different from Vdovichenko's. See R. P. Feynman, *Statistical Mechanics* (Benjamin/Cummings, Reading, MA, 1972), pp. 136–150.

[12]H. N. V. Temperley and M. E. Fisher, Philos. Mag. **6**, 1061 (1961); P. W. Kasteleyn, Physica **27**, 1209 (1961); J. Math. Phys. **4**, 287 (1963); see also McCoy and Wu, Ref. 32.

[13]C. Fan and F. Y. Wu, Phys. Rev. **179**, 560 (1969).

[14]C. Fan and F. Y. Wu, Phys. Rev. B **2**, 723 (1970).

[15]B. Sutherland, J. Math. Phys. **11**, 3183 (1970).

[16]F. Y. Wu, Phys. Rev. Lett. **18**, 605 (1967).

[17]F. Y. Wu, Phys. Rev. **168**, 539 (1968).

[18]See, for example, P. G. Watson, J. Phys. C **1**, 575 (1968); M. E. Fisher, J. Phys. Soc. Jpn. Suppl. **26**, 87 (1969); R. K. P. Zia, Phys. Lett. **64A**, 345 (1978); E. Fradkin, B. A. Huberman, and S. H. Shenker, Phys. Rev. B **18**, 4789 (1978).

[19]A. F. Andreev, Zh. Eksp. Theor. Fiz. **80**, 2042 (1981) [Sov. Phys.—JETP **53**, 1063 (1981)].

[20]C. Jayaprakash and W. F. Saam, Phys. Rev. B **30**, 3916 (1984).

[21]H. A. Kramers and G. K. Wannier, Phys. Rev. **60**, 252 (1941).

[22]M. Kac and J. C. Ward, Phys. Rev. **88**, 1332 (1952).

[23]S. Sherman, J. Math. Phys. **1**, 202 (1960); **4**, 1213 (1963); see also P. N. Burgoyne, *ibid.* **4**, 1320 (1963).

[24]F. Calheiros, S. Johannesen, and D. Merlini, J. Phys. A **20**, 5991 (1987).

[25]This expression is only exact if the interface problem is formulated as done here for a system with fixed boundary conditions such as the strip Ω. If, alternatively, one formulates the interface problem for a system with a pair of "frustrated" plaquettes which are joined by a "seam" of reversed bonds, additional terms appear; however, these additional terms do not contribute to interfacial (order L) properties in the thermodynamic limit, as the separation between the frustrated plaquettes becomes macroscopic.

[26]H. Whitney, Comp. Math. **4**, 276 (1937).

[27]To walk from (0,0) to (N,M), a minimum number of $N_0(N,M)$ steps is necessary. In Ref. 9, the first $N_0(N,M)$ terms of the sum $\sum_{n=0}^{\infty}\mathbf{\Lambda}^n$ were, therefore, explicitly omitted. However, since $\int dk_x \int dk_y \exp[i(k_xN+k_yM)]\mathbf{\Lambda}^P$ is identically zero if $P<N_0(N,M)$ [$\Psi_{\mu\kappa}(x,y;n)=0$ if $n<N_0(N,M)$], we may sum over all non-negative powers of $\mathbf{\Lambda}$, thus obtaining a slightly more aesthetic expression for the ECS.

[28]It may be noticed that the same integrand as in Eq. (13) is obtained by substituting Eq. (12) into Eq. (6) and making a change of variable to $k_y'=k_y+i\beta\lambda X$. We then get the same integrand as a function of k_y' as that which is obtained as a function of k_y by incorporating the field term into $\mathbf{\Lambda}$ from the beginning, except that the integration over k_y' is from

$-\pi+i\beta\lambda X$ to $\pi+i\beta\lambda X$. That this is consistent with Eq. (13) follows simply from the translational invariance of the lattice, which implies that the integrand is invariant under $\mathrm{Re}(k_x,k_y)\rightarrow\mathrm{Re}(k_x,k_y)+(2\pi n,2\pi m)$, with n,m integers. Thus, if we integrate in the k_y' plane along the contour $C=C_1\cup C_2\cup C_3$, where C_1 is the straight line from $i\beta\lambda X$ to $-\pi$, C_2 the straight line from $-\pi$ to π, and C_3 the straight line from π to $i\beta\lambda X$, the contributions from C_1 and C_3 cancel, leaving only the integration along the real axis [Eq. (13)].

[29]$\mathbf{\Lambda}$ is a matrix of exponentials and, therefore, $\mathrm{Det}(\mathbf{1}-\mathbf{\Lambda})$ and $C(\mathbf{\Lambda})\equiv\sum_{i=1}^{q}\prod_{j\neq 1}^{q}(1-\lambda_j)$ are analytic functions of k_x and k_y. The saddle-point condition for (14) is thus found as usual by differentiating $ik_xN+\ln C(\mathbf{\Lambda})-\ln\mathrm{Det}(\mathbf{1}-\mathbf{\Lambda})$ and setting the result equal to zero. That the saddle point is given by $\mathrm{Det}(\mathbf{1}-\mathbf{\Lambda})=0$ is also clear from the fact that the form of $\mathbf{\Lambda}$, combined with the translational invariance of the lattice, implies that $C(\mathbf{\Lambda})$ and $\mathrm{Det}(\mathbf{1}-\mathbf{\Lambda})$ must be polynomials of order $\sim q$ in z and $1/z$, where $z=\exp(ik_x)$. The only contributions to the integral can come from the zeros of $\mathrm{Det}(\mathbf{1}-\mathbf{\Lambda})$.

[30]See, for example, I. Syozi, in *Phase Transitions and Critical Phenomena,* edited by C. Domb and M. S. Green (Academic, New York, 1972), Vol. 1, pp. 269–329, and references therein.

[31]Reading off the equilibrium crystal shape from the bulk free energy will, of course, lead to an ECS for a lattice which has the same basis vectors **a** and **b** as the lattice on which the bulk problem was solved. Let the resulting ECS be given by $\mathrm{Det}[\mathbf{1}-\mathbf{\Lambda}_b(\mathbf{X})]=0$, with $\mathbf{X}=(X,Y)$. If we are interested in a lattice $\mathcal{L}'$ which has basis vectors $\mathbf{a}'=\mathbf{M}\mathbf{a}$ and $\mathbf{b}'=\mathbf{M}\mathbf{b}$, where $\mathbf{M}$ is the matrix of the appropriate linear transformation, then the ECS for the system on $\mathcal{L}'$ is given by $\mathrm{Det}[\mathbf{1}-\mathbf{\Lambda}_b(\mathbf{X}')]=0$, with $\mathbf{X}'=\mathbf{M}^{-1}\mathbf{X}$.

[32]The rectangular Ising model is an example of a model for which it is possible to perform the inversion in closed form. The resulting expression of $\gamma(\theta)$ may be found in Refs. 4.

[33]Rectangular lattice: H. Cheng and T. T. Wu, Phys. Rev. **164**, 719 (1967); see also B. McCoy and T. T. Wu, *The Two dimensional Ising Model* (Harvard, Cambridge, MA, 1973), pp. 299–305. Triangular/honey comb lattice: H. G. Vaidya, Phys. Lett. **57A**, 1 (1976).

[34]K. Kano and S. Naya, Prog. Theor. Phys. **10**, 158 (1953).

[35]V. G. Vaks, A. L. Larkin, and Yu N. Ovchinnikov, Zh. Eksp. Theor. Fiz. **49**, 1180 (1965) [Sov. Phys.—JETP **22**, 820 (1966)].

[36]C. A. Hurst and H. S. Green, J. Chem. Phys. **33**, 1059 (1960); C. A. Hurst, J. Math. Phys. **7**, 305 (1966).

[37]The 3D KDP model was originally proposed by Slater, J. Chem. Phys. **9**, 16 (1941). The 2D KDP model was solved independently by Lieb and Sutherland; see E. H. Lieb, Phys. Rev. Lett. **19**, 108 (1967); B. Sutherland, *ibid.* **19**, 103 (1967).

[38]E. H. Lieb and F. Y. Wu, in *Phase Transitions and Critical Phenomena,* edited by C. Domb and M. S. Green (Academic, New York, 1972), Vol. 1.

[39]G. V. Ryazanov, Zh. Eksp. Teor. Fiz. **59**, 1000 (1970) [Sov. Phys.—JETP **32**, 544 (1971)].

[40]This is slightly different from the traditional picture of an Ising crystal. In the traditional picture, a ferromagnetic Ising model is interpreted as a lattice-gas model of the solid-fluid system for which the ECS problem was originally formulated (Ref. 1). As stated in the Introduction, however, there is nothing sacred about solid-fluid coexistence. The problem of finding the shape of a macroscopic inclusion of one phase in another is well defined whenever the inclusion and the surrounding medium coexist in equilibrium. The problem is particularly interesting when there is crystalline anisotropy, as is the case for coexisting 2×1 phases on the triangular lattice.

[41]In the antiferromagnetic sector, there are real, unbounded solutions $Y(X)$ to $\mathrm{Det}[\mathbf{1}-\mathbf{\Lambda}(X,Y)]=0$ for $X\in[-\infty,X_L]\cup[X_R,\infty]$ even for finite e_1. We believe that these solutions have no physical significance, at least not in the context of ECS's. When $e_1=\infty$, X_L and X_R coincide with the "boundaries" $X_{\min}$ and $X_{\max}$ of the ECS. (For purely ferromagnetic Ising models, no such real, unbounded solutions exist.)

[42]For those orientations θ for which the function $\gamma(\theta)$ defined in Eq. (30) does not contribute to the ECS, $\gamma(\theta)$ is not an interfacial free energy. If $\mathbf{R}=(n,m)$ is not tangent to the ECS, an interface from (0,0) to (n,m) will consist of two macroscopically linear segments in accordance with the lever rule (e.g., Wortis, Ref. 2). The *single* sharp corner thus generated (costing infinite energy, but having zero thermodynamic weight) is strictly disallowed in the calculation leading to (30). Thus only for orientations tangent to the ECS, does (30) have meaning as the interfacial free energy of the modified KDP model.

[43]A.-C. Shi and M. Wortis, Phys. Rev. B **37**, 7793 (1988).

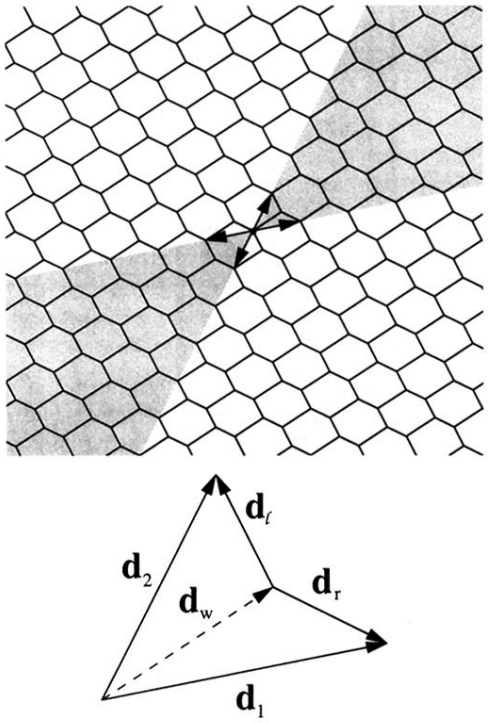

FIG. 10. Feynman-Vdovichenko walker for the modified KDP model performs a very simple walk on the honeycomb lattice: The infiniteness of the interactions forces the walker to make maximal use of the lowest-energy step, which we take to be $\pm\mathbf{d}_w$. Every step $\mathbf{d}_w$ is followed by a step $\mathbf{d}_r$ or $\mathbf{d}_l$ which must be followed again by a step $\mathbf{d}_w$, and so on. Thus the walk takes place effectively on a square lattice with the composite steps $\pm\mathbf{d}_1$ and $\pm\mathbf{d}_2$. Since every composite step must be followed by a composite step of the same sign, only the shaded regions are accessible to a walker starting out at a given lattice site. The fact that directions outside the shaded regions are forbidden is what causes the sharp corners of the ECS of the modified KDP model and gaps in the corresponding Wulff plot.

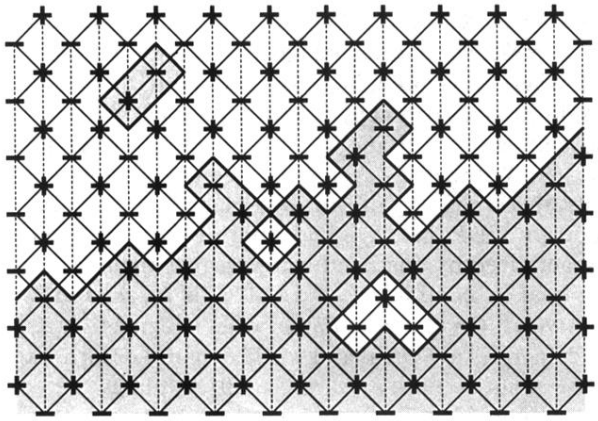

FIG. 7. An interface between two degenerate 2×1 phases of the antiferromagnetic triangular Ising model. The dashed bond is weaker than the others so that the ground state corresponds to spins aligned in rows along the dashed lines.